Copyright © 2007 Tech Science Press CMES, vol.22, no.1, pp.65-76, 2007

Meshless Local Petrov-Galerkin Collocation Method for Two-dimensional Heat Conduction Problems

WU XueHong[1], **SHEN ShengPing**[2] **and TAO WenQuan**[1,3]

Abstract: Meshless local Petrov-Galerkin collocation method is applied to compute two-dimensional heat conduction problems in irregular domain. By taking the Dirac's Delta function as the test function, the local domain integration is avoided. The essential boundary conditions can be implemented easily in this method. A case that has analytical solution shows the present method can obtain desired accuracy and efficient. Two cases in engineering are computed to validate the approach by comparing the present method with the finite volume method (FVM) solutions obtained from a commercial CFD package FLUENT 6.3. The results show that the present method is in good agreement with the FLUENT 6.3, and has very high computational precision. The proposed method, which is a truly meshless method, can describe the boundaries of irregular domain more accurately, and be very easy to be implemented in engineering.

Keyword: meshless method; local Petrov-Galerkin collocation method, least-square approach, heat conduction

1 Introduction

In the past three decades, the finite volume method (FVM) and finite element method (FEM) have been widely applied to compute fluid flow and heat transfer problems. However, these methods depend strongly on the mesh properties. The generation of the good quality meshes is a far more time-consuming and burdensome task, particularly in 3D. At the same time, they have also some drawbacks to solve the problems with shear-band formation, large deformations etc. Owing to these reasons, meshless methods have received much more attention in recent years as a new tool to overcome the above difficulties. In principle, meshless methods rely only on a group of arbitrarily distributed scatter points in the problem computational domain, which can not only alleviate the burdensome to generate mesh, but also describe more accurately the irregular geometries.

In the early stage of the development of the meshless methods, they were usually used in the solid mechanics. In recent years, some authors used the meshless method to solve heat conduction problem. Cleary and Monaghan (1999) applied the smooth particle hydrodynamics (SPH) to solve unsteady-state heat conduction problems. Chen et al. (1999) solved unsteady-state heat conduction problems with a corrective SPH method; Singh and his colleagues (2002, 2003a, 2003b, 2004, 2006) used element-free Galerkin (EFG) method to solve heat conduction problems, and their investigated results shows EFG method results are more accurate than the FEM results. Liu and Yang (2002) applied the EFG method and the EFG-FEM to solve the heat conduction problems. Sladek et al. (2004a) applied MLPG method to solve the heat conduction problem in an anisotropic medium. Liu et al. (2005) uses meshless weighted least-squares (MWLS) method to solve steady- and unsteady-state heat conduction problems. Tan et al. (2006) applied least-squares collocation meshless method to solve coupled radiative and heat conduction problems. Sadat et al. (2006) used DAM to solve a two-dimensional heterogeneous heat conduction problem.

[1] State Key Laboratory of Multiphase Flow in Power Engineering, School of Energy and Power Engineering, Xi'an Jiaotong University, Xi'an, Shanxi 710049, PR China
[2] MOE Key Laboratory for Strength and Vibration, School of Aerospace, Xi'an Jiaotong University, Xi'an, Shanxi 710049, PR China
[3] Email: wqtao@mail.xjtu.edu.cn

Previous researchers have focused mainly on using EFG method and SPH method to solve the heat conduction problems. However these methods need numerical integration to compute partial differential equations (PDEs), they are more time-consuming. Meanwhile, almost all of the previous works limit to heat conduction problems of regular domain. However, many problems in engineering are in irregular domain, and FVM and FEM are difficult to describe accurately boundaries of the irregular domain unless the mesh is very fine, or special grid generation method is adopted which is usually time-consuming. Meshless methods can overcome this difficulty because they do not need mesh. Meshless methods distribute arbitrarily scattering points in the problem domain, so they will have more advantage in solving problems with irregular domain than FVM and FEM. The MLPG method, a truly meshless method developed by Atluri and his colleagues, is a simple and less-costly alternative to the FEM and FVM [Atluri and Zhu (1998), Atluri and Shen (2002a, b)]. Remarkable successes of the MLPG method have been reported [Sladek, et al.. (2004b); Han and Atluri (2004a, b); Atluri and Shen (2005); Han, et al.. (2005, 2006); Atluri, et al.. (2004, 2006a, b); Liu, et al.. (2006)]. Although meshless methods possess several advantages, one of its major difficulties is the numerical integration. To avoid this difficulty, Alturi and Shen (2002a, b) and Atluri (2004) choose the collocation Dirac's Delta function to be the test function in MLPG methods. This kind of meshless local Petrov-Galerkin method uses a local asymmetric weak-form for which no numerical integration is needed and the solution is independent of the size of the support of the test function. The computational effort of this method is less than those of the EFG, SPH and other MLPG methods.

In this paper, we apply meshless local Petrov-Galerkin (MLPG) collocation method to solve two steady-state heat conduction problems with irregular domain in engineering. The moving least-squares approximation is used to construct the shape functions. A case that has analytical solution is employed to verify efficiency and accuracy of the present method, and the results of two problems with irregular domain are compared with FVM solutions generated by FLUENT 6.3.

2 The Moving Least-Square (MLS) Approximation Scheme

In order to preserve the local character of the numerical implementation, the MLPG collocation method needs some kind of interpolation schemes and discretization methods to generate the algebraic equations, which can be solved numerically. There are a number of local interpolation schemes, such as MLS, Partition of Unity Method (PUM), Shepard function, Reproducing Kernel Particle Method (RKPM), etc. In the present paper, we utilize MLS method as interpolation scheme. The characteristic of MLS has been widely discussed in literatures [Alturi and Zhu (1998), Jin et al. (2001)], and will not be restated here.

Consider a function $T^h(x)$ defined in a sub-domain Ω_X, which is discretized by a set of field nodes x_I $(I = 1,\ldots N)$ (see Fig.1). The moving least squares approximate $T^h(x)$ by $T(x)$, can be defined by

$$T(x) \approx T^h(x) = \sum_{i=1}^{m} p_i(x)a_i(x) = \mathbf{p}^{\mathrm{T}}(\mathbf{x})\mathbf{a}(\mathbf{x}) \tag{1}$$

where $p_i(x)$ is a complete monomial basis in the space that co-ordinate $X^{\mathrm{T}} = [x,y]$, m is the number of terms in the basis; $a_i(x)$ is the corresponding coefficient. The coefficient vector $\mathbf{a}(\mathbf{x})$ is determined by minimizing the difference between the local approximation and the function, which is defined as:

$$\begin{aligned} J(\mathbf{a}(\mathbf{x})) &= \sum_{I=1}^{N} w_I(x)\left[T^h(x_I) - \hat{T}^I\right]^2 \\ &= \sum_{I=1}^{N} w_I(x)\left[\mathbf{p}^{\mathrm{T}}(\mathbf{x}_I)\mathbf{a}(\mathbf{x}) - \hat{T}^I\right]^2 \end{aligned} \tag{2}$$

where: x_I denotes the position vector of node I; $w_I(x)$ is the weight function associated with the node x_I; N is the number of node in Ω_x, and $\hat{T}^I = T(x_I)$ is the fictitious nodal value. It is not the nodal value of trial functions denoted by $T^h(x)$.

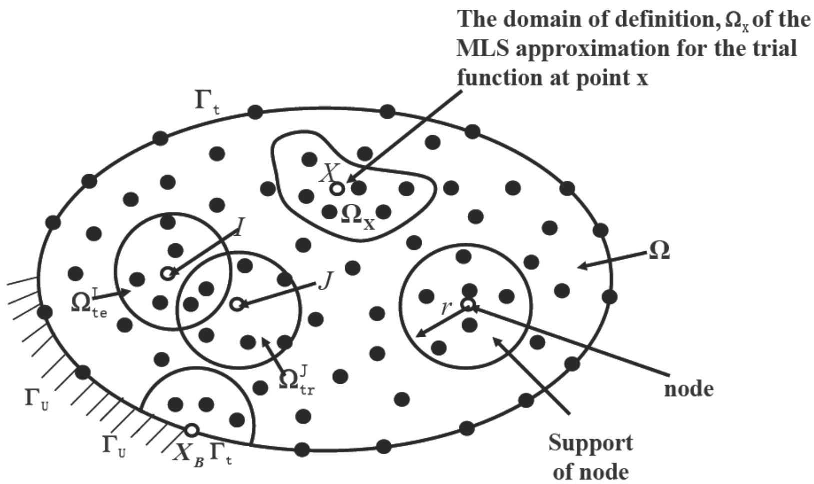

Figure 1: Schematics of the MLS approximation

To find the coefficient $\mathbf{a}(\mathbf{x})$, we obtain the extremum by

$$\frac{\partial J(\mathbf{a}(\mathbf{x}))}{\partial(\mathbf{a}(\mathbf{x}))} = 2\sum_{I=1}^{N} w_I(x)\left[\sum_{i=1}^{m} p_i(x_I)a(x) - \hat{T}^I\right]p_i(x_I) = 0 \tag{3}$$

This leads to the following set of linear relations.

$$\mathbf{A}(\mathbf{x})\mathbf{a}(\mathbf{x}) = \mathbf{B}(\mathbf{x})\hat{\mathbf{T}} \tag{4}$$

where the matrices $\mathbf{A}(\mathbf{x})$ and $\mathbf{B}(\mathbf{x})$ are defined by:

$$\begin{aligned}\mathbf{A}(\mathbf{x}) &= \mathbf{P}^{\mathrm{T}}\mathbf{W}\mathbf{P} = \mathbf{B}(\mathbf{x})\mathbf{P}\\ &= \sum_{I=1}^{N} w_I(x)\mathbf{p}(\mathbf{x_I})\mathbf{p}^{\mathrm{T}}(\mathbf{x_I})\end{aligned} \tag{5}$$

$$\begin{aligned}\mathbf{B}(\mathbf{x}) &= \mathbf{p}^{\mathrm{T}}\mathbf{w}\\ &= [w_1(x)\mathbf{p}(\mathbf{x_2}), w_2(x)\mathbf{p}(\mathbf{x_2}), \ldots w_3(x)\mathbf{p}(\mathbf{x_3})]\end{aligned} \tag{6}$$

$$\hat{T}^{\mathrm{T}} = \left[\hat{T}^1, \hat{T}^2, \ldots, \hat{T}^N\right] \tag{7}$$

Solving $\mathbf{a}(\mathbf{x})$ from Eq. (4), and substituting it into Eq. (1), we can obtain the final form of the MLS approximation as:

$$T^h(x) = \mathbf{\Phi}^{\mathrm{T}}(\mathbf{x}) \cdot \hat{\mathbf{T}} = \sum_{I=1}^{N} \phi(x)\hat{T}^I \quad x \in \Omega_x \tag{8}$$

where $\mathbf{\Phi}^{\mathrm{T}}(\mathbf{x}) = \mathbf{p}^{\mathrm{T}}(\mathbf{x})\mathbf{A}^{-1}(\mathbf{x})\mathbf{B}(\mathbf{x})$ is the shape function. The partial derivatives of such shape function can be obtained from literature [Liu and Gu (2005)], and will be omitted here for simplicity.

The smoothness of the nodal shape function $\phi^I(x)$ is determined by the basis and the weight function. The quadratic basis is selected. The weight function $w_I(x)$ is generally nonzero over the small neighborhood points of x_I, called the domain of influence of node I (see Fig. 1). The choice of weight function $w_I(x)$ affects the resulting approximation $T^h(x)$; therefore its selection is of essential importance. Numerical practices have shown [Atluri and Zhu (1998), Singh (2004)] that a quadratic spline weight function works well. Hence in this article, the quadratic spline weight function is used. Thus we have:

$$w_I(x) = \begin{cases} 1 - 6D_I^2 + 8D_I^3 - 3D_I^4 & 0 \le D_I \le 1 \\ 0 & D_I > 1 \end{cases} \tag{9}$$

where $D = \sqrt{(x-x_I)^2 + (y-y_I)^2}/r$, and r is the size of support for the weight functions.

3 Numerical Implementation of the MLPG Collocation Method

The steady-state heat conduction with inner source and the related boundary conditions can be written as:

Poisson equation:

$$\lambda \cdot \nabla^2 T = \dot{\Phi} \quad \text{in } \Omega \tag{10}$$

The Dirichlet boundary condition:

$$T = T_1 \quad \text{on } \Gamma_1 \tag{11}$$

The Neumann boundary condition:

$$-\lambda \nabla T \cdot n_j = q \quad \text{on } \Gamma_2 \tag{12}$$

The Robbin boundary condition:

$$\lambda \nabla T \cdot n_j = h(T_f - T) \ \text{ on } \Gamma_3 \tag{13}$$

where, T represents the temperature, λ is thermal conductivity, n_j is the outward unit vector to Γ, q is given heat flux, h is the convection heat transfer coefficient, t_f is the environmental temperature, $\dot{\Phi}$ is the heat source per unit mass, Γ_1, Γ_2 and Γ_3 denote the boundaries at which the three kinds of boundary conditions (Dirichlet, Neumann and Robin conditions)are applied, respectively.

The weighted integral form of Eq. (10) is given as

$$\int_{\Omega_x} \left[\lambda \nabla^2 T - \dot{\Phi}\right] v d\Omega_x = 0 \tag{14}$$

We use the collocation Dirac's Delta function $\delta(x - x_I)$ as the test function in each Ω_x. Substituting the Dirac's Delta function $\delta(x - x_I)$ into the above equation, we can obtain:

$$\lambda \nabla^2 T(x_I) - \dot{\Phi}(x_I) = 0, \quad (I = 1, \ldots, M) \tag{15}$$

Substituting the interpolation (8) into Eq. (15) for the internal nodes, and boundary conditions (11-13), leads to the following discretized system of linear equations:

$$\sum_{J=1}^{M} \phi^J_{,ii}(x_I)\hat{T}^I = \dot{\Phi}(x_I) \quad \text{for interior nodes} \tag{16a}$$

$$\sum_{J=1}^{M} \phi^J(x_I)\hat{T}^J = T_1(x_I) \quad \text{on } \Gamma_1 \tag{16b}$$

$$-\sum_{J=1}^{M} \frac{\partial \phi^J(x_I)}{\partial n}\hat{T}^J = q(x_I) \quad \text{on } \Gamma_2 \tag{16c}$$

$$\sum_{J=1}^{M} \frac{\partial \phi^J(x_I)}{\partial n}\hat{T}^J = h\left(T_f(x_I) - \phi^J(x_I)\hat{T}^J\right) \quad \text{on } \Gamma_3 \tag{16d}$$

where $I = 1, \ldots, M$. Eq. (16) can be rewritten as

$$\mathbf{K} \cdot \hat{\mathbf{T}} = \mathbf{F} \tag{17}$$

where, M is the total number of nodes in the entire domain Ω, $\hat{\mathbf{T}}$ is the vector for the unknown fictitious nodal values, $\hat{\mathbf{T}} = [\hat{T}^1, \hat{T}^2 \cdots \hat{T}^M]$, and $\mathbf{K}$ and $\mathbf{F}$ are the global stiffness matrix and the global vector, respectively, which are defined as:

$$K_{IJ} = \begin{cases} \phi^J_{,ii}(x_I) & x_I \in \Omega \\ \phi^J(x_I) & x_I \in \Gamma_1 \\ -\phi^J_{,n}(x_I) & x_I \in \Gamma_2 \\ \phi^J_{,n}(x_I) + h \cdot \phi^J(x_I) & x_I \in \Gamma_3 \end{cases} \tag{18}$$

and

$$f_I = \begin{cases} \dot{\Phi}(x_I) & x_I \in \Omega \\ T_1(x_I) & x_I \in \Gamma_1 \\ q(x_I) & x_I \in \Gamma_2 \\ hT_f(x_I) & x_I \in \Gamma_3 \end{cases} \tag{19}$$

here $I, J = 1, \ldots, M$. M is the total nodes .

4 Numerical Examples

In this section, we apply the above method to solve a problem that has analytical solution to illustrate the accuracy and efficiency. Then we apply the present method to compute two problems of heat conduction in irregular domain in engineering. Two examples are employed to validate the formulation by comparing the meshless results to finite volume method (FVM) solutions provided by the commercial CFD package FLUENT 6.3.

4.1 Patch Test

A square domain in the dimension 1m×1m is shown in Figure 2. Its right boundary is given heat transfer coefficient h = 5W/(m^2·°C) and the surrounding temperature T_f = 0°C. The upper boundary and left boundary are adiabatic, and the bottom boundary is maintained at the temperature T_w = 1°C. There is no heat source in the domain. The thermal conductivity is λ = 1W/(m°C). The analytical solution is given by

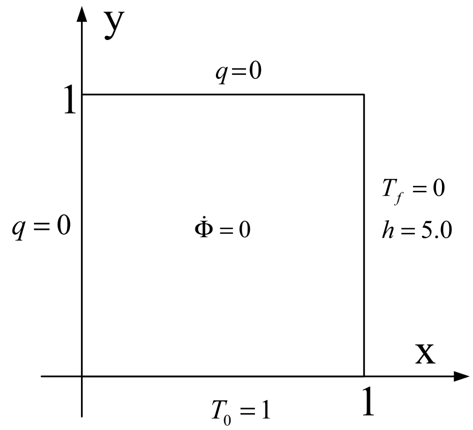

Figure 2: Problem description for patch test

Necatiözisik (1980):

$$T(x,y) = 2T_0 h \sum_{m=1}^{\infty} \frac{1}{(\beta_m^2 + h^2) + h} \frac{\cosh \beta_m (1-y)}{\cosh \beta_m} \cdot \frac{\cos \beta_m x}{\cos \beta_m} \quad (20)$$

where, β_m is the positive solution of the equation $\beta_m \tan \beta_m = h$.

The relative error of the numerical solution is defined as

$$Er = \frac{\|T^{num} - T^a\|}{\|T^a\|} \quad (21)$$

where the superscripts num denotes the numerical results of MLPG collocation method or FVM, a denotes analytical solutions, and N is the total node.

The relative error is shown in Figure 3, where D is node distance. It can be seen that MLPG collocation method is more accurate than the finite volume method (FVM). In this patch test, we use a uniform node of $21\times21(441)$ collocation point. The influence of the sizes of local support domain is shown in Figure 4; when a support domain is too small or too large, the relative error will become unacceptably large; $r = 2.5 - 3.0$ is an economical choice that gives good results. In this patch test and following two cases, we select a support size of 2.5 times of the nodal distance (Liu and Gu (2005)), and the quadratic basis is used in the MLPG collocation method. To compare the computational effort required for the MLPG collocation method with FVM, the problem is recomputed for cases of different nodes in an AMD 3800+ computer. The computational time required is listed in Tables 1 and 2. From Table 1 it can be seen that this method need two times computational cost than the FVM at the same nodal distance ($D = 0.05$). However, for the same accuracy (Table 2), this method need less nodes than the FVM, and the CPU time of this method is the same as that of the FVM. Some discussion on the comparison of computational time is added here. Theoretically speaking, the solution of meshless method should need less computational time than that from FVM or FEM, because the saving in CPU time for grid generation. And this advantage of meshless method will become more and more appreciable with the increase in the complexity of solution domain. However, for the present case solution domain is the simplest one. In addition, meshless method is still in its early development stage, while FVM can be regarded as well developed. Commercial code such as FLUENT has been used for many years, and its code structure and algorithm are well organized and even optimized, while our program of meshless method has just been coded without further improvement in code design. Considering the above-mentioned aspects, it should be acceptable at the present stage when comparison results of computational time of meshless method to the conventional method do not show appreciable saving in time or even more time-consuming in some extent.

Figure 5 gives predicted temperature fields and Figure 6 gives predicted temperature distributions along the two centerlines ($x = 0.5$ and $y = 0.5$). From Figures 5 and 6, we can see that the result from MLPG collocation method and FVM agree very well with the results of analytical solution. It also shows that the MLPG collocation method is an efficient and accurate numerical method.

4.2 Heat Conduction in Insulation Layer of Tube Transporting Vapor

The pipe for transporting vapor with a diameter 200mm is covered by thermal insulation layer

Table 1: Computational time required (s) in $D = 0.05$ and relative error

Scheme	CPU time (s)	Relative error (%)
MLPG collocation method	0.14	0.06
FVM	0.06	0.1

Table 2: The node numbers and CPU times for the same accuracy

Scheme	Node numbers	CPU time (s)
MLPG collocation method	16×16	0.06
FVM	22×22	0.06

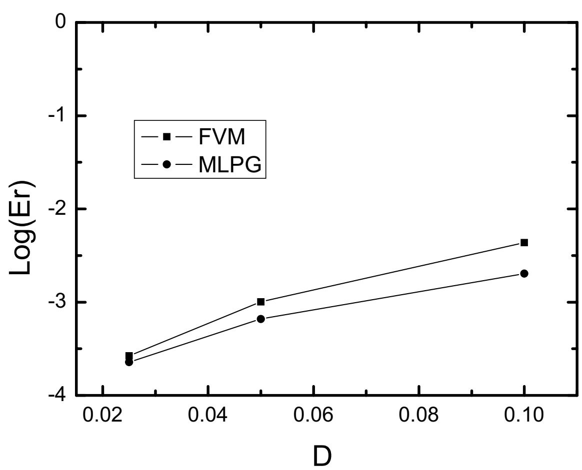

Figure 3: Relative errors for patch test

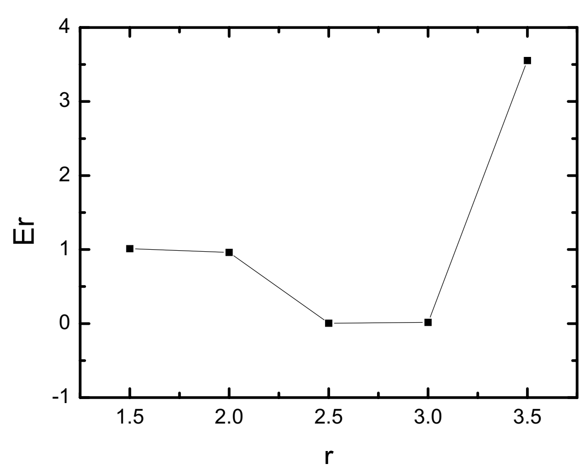

Figure 4: Influence of the sizes of local support domain for patch test

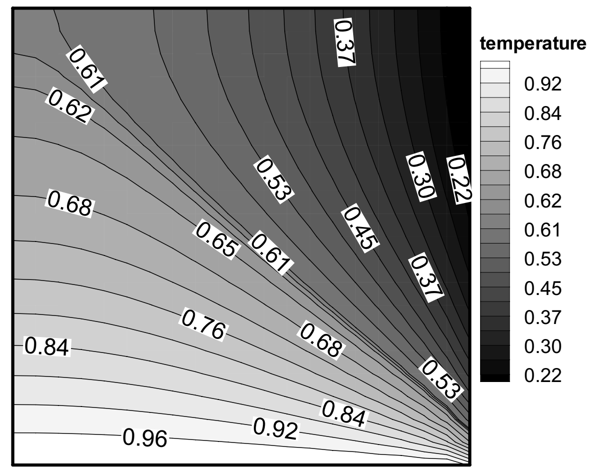

(a) Analytical solution

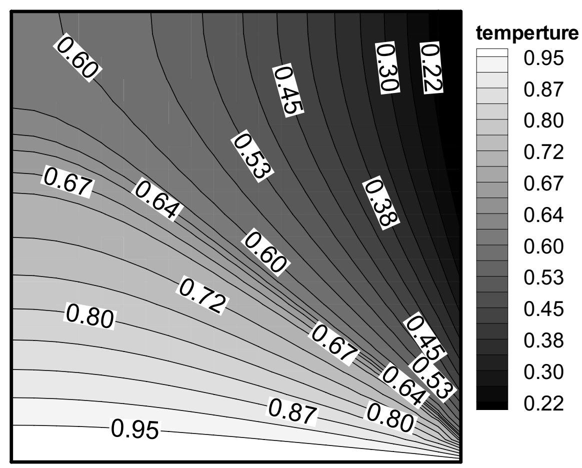

(b) MLPG collocation method

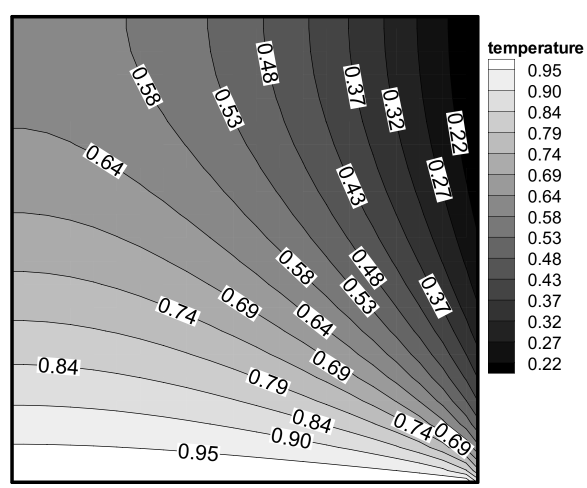

(c) FVM

Figure 5: Comparison temperature fields for patch test (^{o}C)

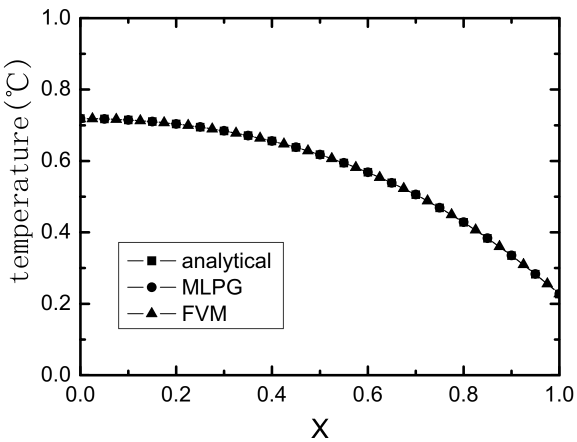

(a) Temperature distribution along $y = 0.5$

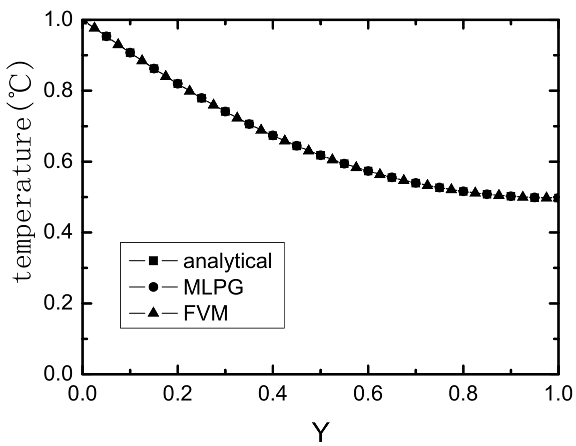

(b) Temperature distribution along $x = 0.5$

Figure 6: Comparison temperature distribution for patch test (°C)

with a square structure of 400mm×400mm, as shown in Figure 7. Inter surface and outer surface temperature of heat insulation layer is maintained at the temperature $T_1 = 200^o$ and $T_2 = 60^o$, respectively. Thermal conductivity of thermal insulation layer is $\lambda = 0.1$W/(m°C). Due to symmetry, only the shadow region is selected as the computational domain.

Node discretization of MLPG collocation method and mesh of FVM are shown in Figure 8. Node independency test of the present method is shown in Figure 9 by comparing the temperature distribution along the line 1 in Figure 8 (b), and it can be seen that the number of 336(21×16) collocation points can obtain very good results. The computational method and boundary conditions treatment

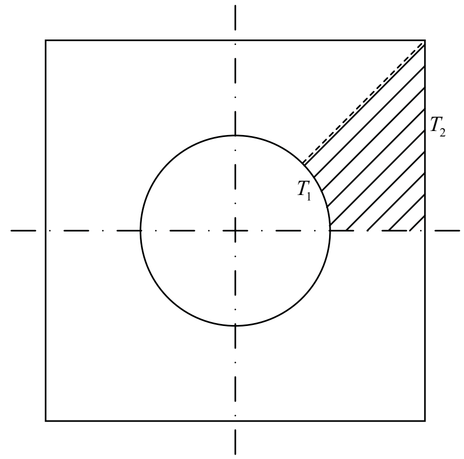

Figure 7: Physical model and computational domain for heat conduction in insulation layer of tube transporting vapor

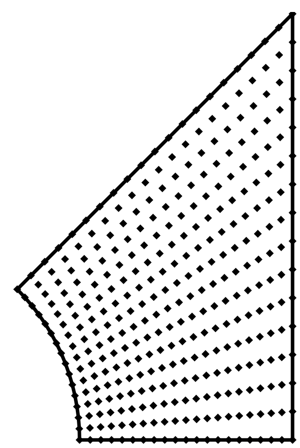

(a) MLPG collocation method

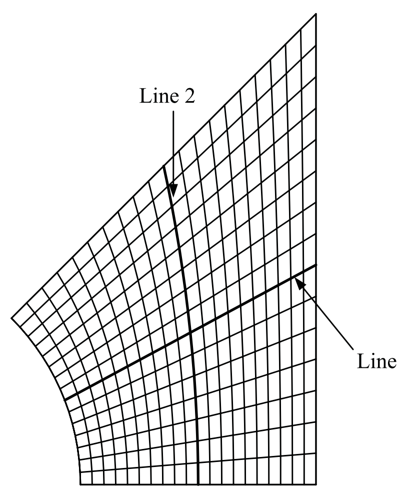

(b) FVM

Figure 8: Node or mesh distribution for heat conduction in insulation layer of tube transporting vapor

are the same as the above case. Figure 10 and Figure 11 give the predicted temperature fields and temperature distributions along line 1 and line 2 (see Fig.8 (b)) from the present method and FVM, respectively. The results of the present method are in very good agreement with those obtained using FVM. The CPU time of this method and FVM are give in the Table 3 for the same node numbers; It can be seen that for the problem studied this method require a bit more computational time. The possible reasons have been discussed above.

Table 3: Computational time required (s) for heat conduction in insulation layer of tube transporting vapor

Scheme	CPU time (s)
MLPG collocation method	0.09
FVM	0.07

4.3 Heat Conduction in Conduction Mud

In the petrochemical engineering, in order to transport high viscosity material such as petroleum, it often adopts vapor heating system to keep the tube side bitumen at certain temperature, which can efficiently decrease the its viscosity . In recent years, a kind of new material (conduction mud) which has higher thermal conductivity is employed. It is filled between a heating pipe and a heated pipe (see Figure 12), and can significantly enhance heat transfer between them (Chen et al. (2001)). The heat conduction within the conduction mud is now simulated by the present meshless method. The thermal conductivity of the conduction mud is $\lambda = 10\text{W/(m}^{\text{o}}\text{C)}$, the outer surfaces of the two pipes are maintained at the temperature 150$^{\text{o}}$C and 100$^{\text{o}}$C, respectively. Due to symmetry, only the right half of shadow domain is modeled.

Node discretization of MLPG collocation method and mesh of FVM are shown in Figure 13. Node independency test of the present method is shown in Figure 14 by comparing the temperature distribution along the line 1 in Figure 13(b). It can be seen that the number of 336(21×16) collocation

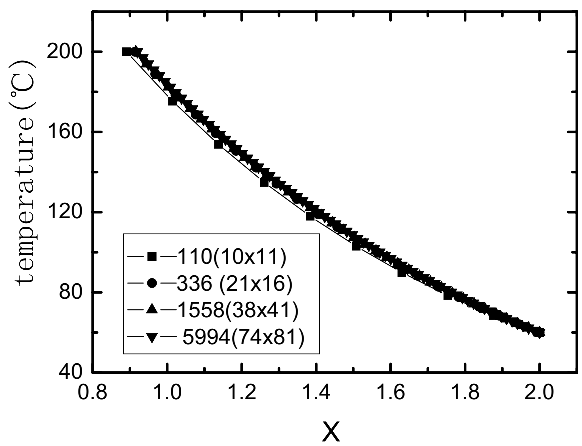

Figure 9: Node independency test for heat conduction in insulation layer of tube transporting vapor

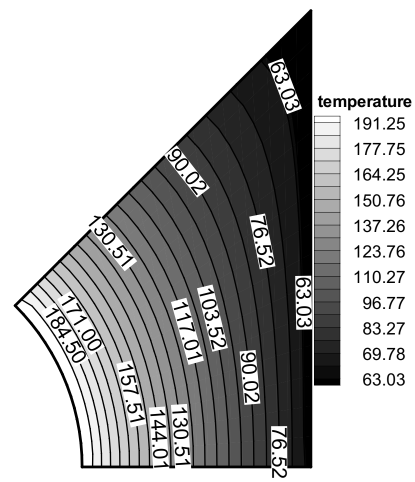

(a) FVM

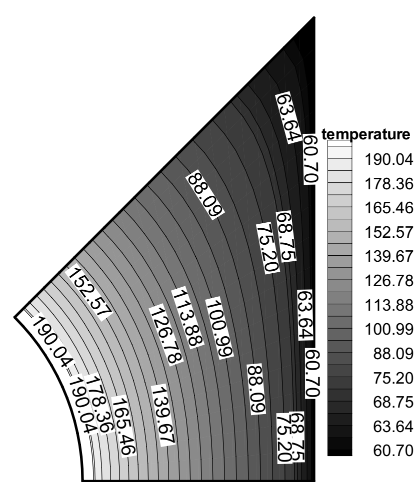

(b) MLPG collocation method

Figure 10: Comparison temperature fields for heat conduction in insulation layer of tube transporting vapor ($^{\text{o}}$C)

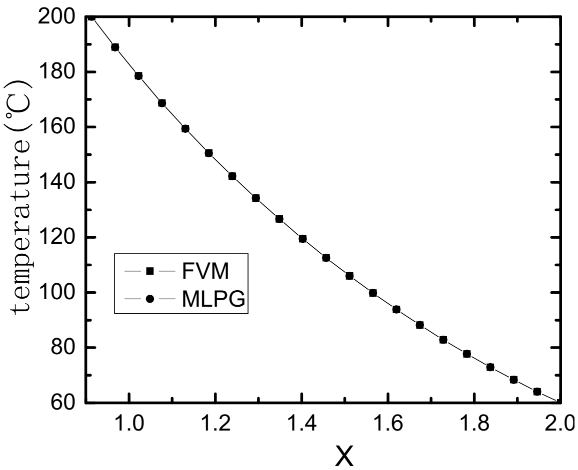

(a) Temperature distribution along line 1

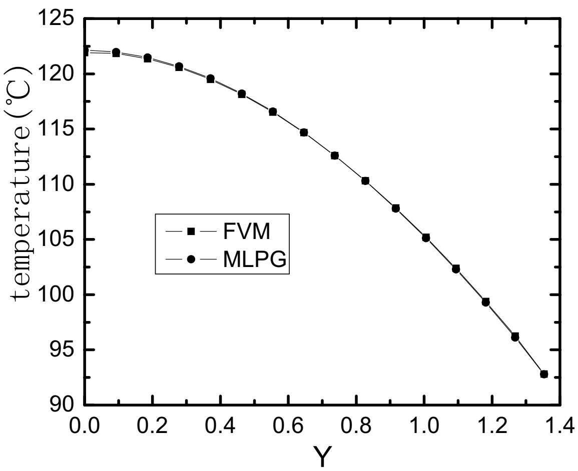

(b) Temperature distribution along line 2

Figure 11: Comparison temperature distributions for heat conduction in insulation layer of tube transporting vapor (^{o}C)

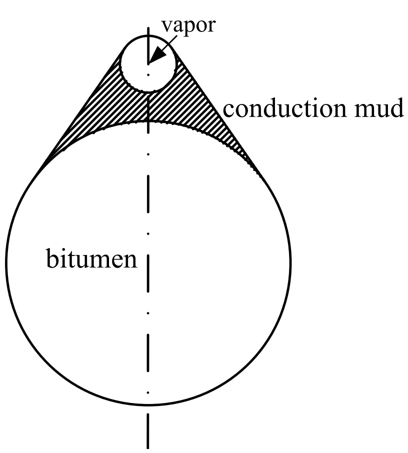

Figure 12: Physical model and computational domain for heat conduction in conduction mud

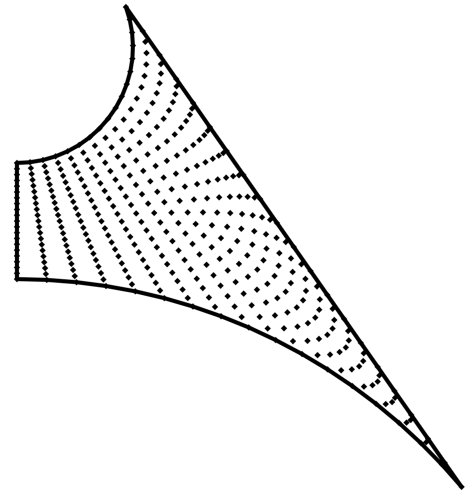

(a) MLPG collocation method

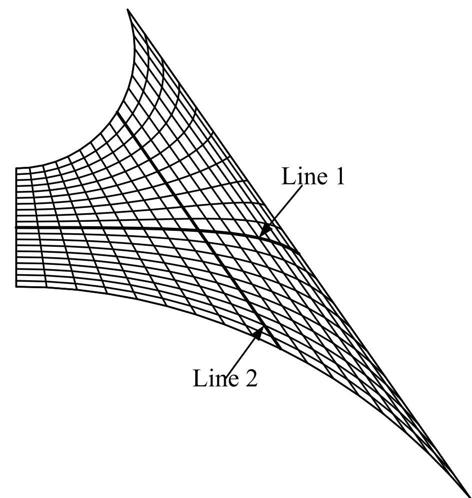

(b) FVM

Figure 13: Node or mesh distribution for heat conduction in conduction mud

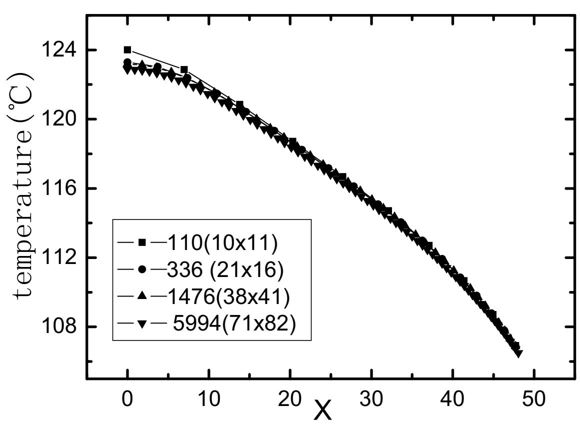

Figure 14: Node independency test for heat conduction in conduction mud

points can obtain very good results. The computational method and boundary conditions treatment are the same as the above case. Figure 15 and Figure 16 give predicted temperature fields and temperature distributions in line 1 and line 2 (see Fig.13 (b)) of the present method and FVM, respectively. Comparisons of the two results show that they are quite close to each other. The CPU time of this method and FVM are give in Table 4 for the same node numbers; it can be seen that this method need less CPU time than that of FVM.

Table 4: Computational time required (s) for heat conduction in conduction mud

Scheme	CPU time (s)
MLPG collocation method	0.12
FVM	0.15

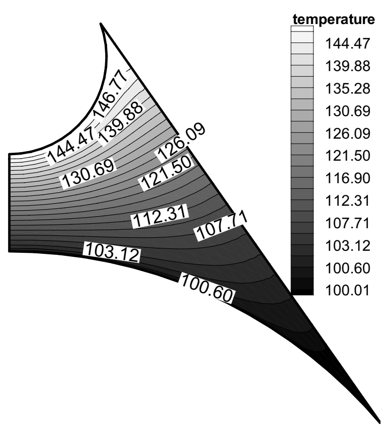

(a) FVM

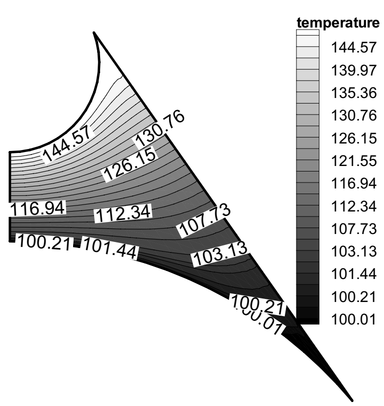

(b) MLPG collocation method

Figure 15: Comparison temperature fields for heat conduction in conduction mud (^{o}C)

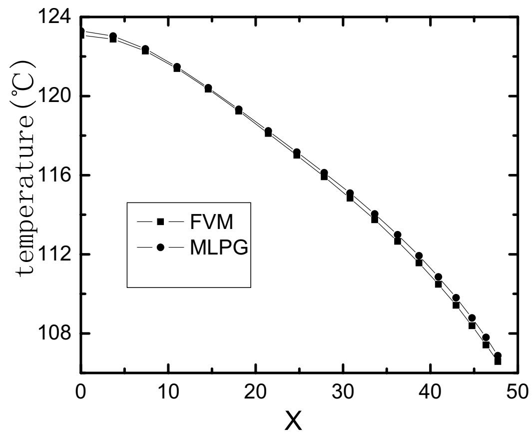

(a) Temperature distribution along line 1

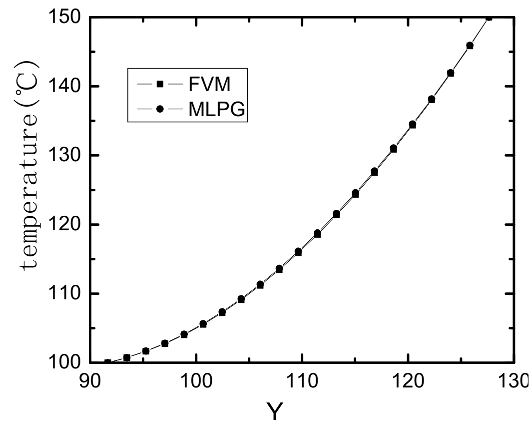

(b) Temperature distribution along line 2

Figure 16: Comparison temperature distributions for heat conduction in conduction mud

5 Discussion and Conclusions

In this paper, the MLPG collocation method has been extended to solve the two-dimensional steady-state heat conduction problems in irregular domain. This method does not need numerical integration; hence it spends less computational time. Moreover, it can describe the boundary of irregular domain more accurately. The numerical results demonstrate the high accuracy of the present method. The results from the present method are in very good agreement with the results from FVM using FLUENT. It is easy to be implemented and has high computational efficiency. Thus the present meshless method sheds light on effectively handling the problems with irregular domain.

Acknowledgement: The project is supported by the National Natural Science Foundation of China (50636050 and 10672130).

References

Atluri, S. N. (2004): *The Meshless Method (MLPG) for Domain & BIE Discretizations*, Tech Science Press, Forsyth, GA.

Atluri, S. N.; Shen, S. (2002a): The Meshless Local Petrov-Galerkin (MLPG) Method: A Simple & Less Costly Alternative to the Finite Element and Boundary Element Methods, *CMES: Computer Modeling in Engineering & Sciences*, 3, 11-52.

Atluri, S. N.; Shen, S. (2002): *The Meshless Local Petrov-Galerkin (MLPG) Method*, Tech Science Press. Encino USA.

Atluri, S. N.; Shen, S. (2005): Simulation of a 4th Order ODE: Illustration of Various Primal & Mixed MLPG Methods, *CMES: Computer Modeling in Engineering & Sciences*, 7, 241-268.

Atluri, S. N.; Han, Z. D.; Rajendran, A. M. (2004): A New Implementation of the Meshless Finite Volume Method, Through the MLPG "Mixed" Approach, *CMES: Computer Modeling in Engineering & Sciences*, 6, 491-514.

Atluri, S. N.; Liu, H. T.; Han, Z. D. (2006a): Meshless Local Petrov-Galerkin (MLPG) Mixed Collocation Method For Elasticity Problems, *CMES: Computer Modeling in Engineering & Sciences*, 14, 141-152.

Atluri, S. N.; Liu, H. T.; Han, Z. D. (2006b): Meshless Local Petrov-Galerkin (MLPG) Mixed Finite Difference Method for Solid Mechanics, *CMES: Computer Modeling in Engineering & Sciences*, 15, 1-16.

Atluri, S. N.; Zhu, T. L. (1998): A New Meshless Local Petrov-Galerkin (MLPG) Approach in Computational Mechanics, *Comput. Mech.*, 22, 117-127.

Chen, C. R; Hu, Y. D; Zhao, C. Y.; Wang, Q. W.; Tao, W. Q. (2001): Numerical Study on Heat Transfer Characteristic of Conduction Mud, *Journal of engineering thermophysics* (China), 22(1), 101-103.

Chen, J. K.; Beraun, J. E.; Carney, T. C. (1999): A Corrective Smoothed Particle Method for Boundary Value Problems in Heat Conduction, *Int. J. Numer. Meth. Engrg.*, 46, 231-252.

Cleary, P. W.; Monaghan, J. J. (1999): Conduction Modeling using Smoothed Particle Hydrodynamics, *J. Comput. Phys.*, 148, 227-264.

Han, Z. D.; Atluri, S. N. (2004a): Meshless Local Petrov-Galerkin (MLPG) Approaches for Solving 3D Problems in Elasto-Statics, *CMES: Computer Modeling in Engineering & Sciences*, 6, 169-188.

Han, Z. D.; Atluri, S. N. (2004b): A Meshless Local Petrov-Galerkin (MLPG) Approach for 3-Dimensional Elasto-dynamics. *CMC: Computers, Materials & Continua*, 1, 129-140.

Han, Z. D.; Rajendran, A. M.; Atluri, S. N. (2005): Meshless Local Petrov-Galerkin (MLPG) Approaches for Solving Nonlinear Problems with Large Deformations and Rotations, *CMES: Computer Modeling in Engineering & Sciences*, 10, 1-12.

Han, Z. D.; Liu, H. T.; Rajendran, A. M.; Atluri, S. N. (2006): The Applications of Meshless Local Petrov-Galerkin (MLPG) Approaches in High-Speed Impact, Penetration and Perforation Problems, *CMES: Computer Modeling in Engineering & Sciences*, 14, 119-128.

Jin, X.; Li, G.; Aluru, N. R. (2001): On the Equivalence between Least-Square and Kernal Approximations in Meshless Methods, *CMES: Computer Modeling in Engineering & Sciences*, 2(4), 447-462.

Liu, H. T.; Han, Z. D.; Rajendran, A. M.; Atluri, S. N. (2006): Computational Modeling of Impact Response with the RG Damage Model and the Meshless Local Petrov-Galerkin (MLPG) Approaches, *CMC: Computers, Materials & Continua*, 4, 43-54.

Liu, R. G.; Gu, Y. T. (2005): *An Introduction to Meshfree Methods and Their Programming*, Springer-Verlag press, Berlin.

Liu, Y.; Yang, H. T. (2002): A Combined Approach of EFG/EF-EFG methods and Precise Algorithm in Time Domain Solving Heat Conduction Problems, *J. Basic Sci. Eng.*(China), 10, 307-

317.

Liu, Y.; Zhang, X.; Liu, M. W. (2005): A Meshless Method Based on Least-Squares Approach for Steady and Unsteady State Heat Conduction Problems, *Numer. Heat Transfer*, Part B, 47, 257-275.

Necatiözisik, M. (1980): *Heat conduction*, New York: Wiley.

Sadat, H.; Dubus, N.; Gbahoue, L.; Sophy, T. (2006): On the Solution of Heterogeneous Heat Conduction Problems by A Diffuse Approximation Meshless Method, *Numer. Heat Transfer*, Part B, 50, 491-498.

Singh, I. V. (2004): A Numerical Solution of Composite Heat Transfer Problems using Meshless Method, *Int. J. Heat Mass Transfer*, 47, 2123-2138.

Singh, I. V.; Prakash, R. (2003a): The Numerical Solution of Three-Dimensional Transient Heat Conduction Problems using Element Free Galerkin Method, *Int. J. Heat Tech.*, 21, 73-80.

Singh, I. V.; Sandeep, K.; Prakash, R. (2002): The Element Free Galerkin Method in Three-Dimensional Steady State Heat Conduction, *Int. J. Comput. Eng. Sci.*, 3, 291-303.

Singh, I. V.; Sandeep, K.; Prakash, R. (2003b): Heat Transfer Analysis of Two-Dimensional Fins using Meshless Element-Free Galerkin Method, *Numer. Heat Transfer*, Part A, 44, 73-84.

Singh, A.; Singh, I. V.; Prakash, R. (2006): Numerical Solution of Temperature-Dependent Thermal Conductivity Problems using A Meshless Mtheod, *Numer. Heat Transfer*, Part A, 50, 125-145.

Sladek, J.; Sladek, V.; Atluri, S. N. (2004a): Meshless Local Petrov-Galerkin Method for Heat Conduction Problem in An Anisotropic Medium, *CMES: Computer Modeling in Engineering & Sciences*, 6(3), 309-318.

Sladek, J.; Sladek, V.; Atluri, S. N. (2004b): Meshless Local Petrov-Galerkin Method in Anisotropic Elasticity. *CMES: Computer Modeling in Engineering & Sciences*, 6, 477-490.

Tan, J. Y.; Liu, L. H.; Li, B. X. (2006): Least-Squares Collocation Meshless Approach for Coupled Radiative and Conductive Heat Transfer, *Numer. Heat Transfer*, Part B, 49, 179-195.